Reconfigurable LPV Control Design for Boeing 747-100/200 Longitudinal Axis

Subhabrata Ganguli *, Andrés Marcos †, Gary Balas ‡
University of Minnesota

Abstract

This paper presents the design of a reconfigurable Linear Parameter Varying (LPV) controller for the Boeing 747-100/200 longitudinal axis in the Up-and-Away flight regime. The control objectives are to obtain decoupled flight-path angle and velocity command tracking and achieve good disturbance rejection characteristics during normal operation and in the presence of an elevator fault.

The LPV controller is synthesized using a quasi-LPV model of the aircraft longitudinal axis based on the Jacobian Linearization approach. The controller schedules on three parameters: flight altitude and velocity, which are available as measurements, and a fault identification signal generated by a fault detection and isolation (FDI) algorithm. During normal flight operations, the LPV controller uses the elevators and thrust for flight maneuvers. The stabilizer is used to trim the aircraft. Two elevator fault scenarios are contemplated — lock and float. The proposed control strategy is to use the stabilizer (normally used for trim purposes only) as the alternative longitudinal control surface. Simulation results with elevator faults present show that the reconfigured controller stabilizes the faulted system at the expense of a factor of a designed one-third reduction in the tracking responsiveness of the longitudinal axis and has good disturbance rejection properties.

1 Introduction

Fault tolerant control systems are an important area of research in flight controls and has become more significant for commercial aviation after US federal government declaring safety of commercial aviation a top priority issue. The national mission to decrease the commercial aviation accident rate by 80% within the next 10 years[1] has motivated researchers to come up with control strategies ensuring adequate failure mitigation.

In general, a fault tolerant flight control system is required to perform failure detection, identification and accommodation for sensor and actuator failures. Fault tolerant control schemes can be broadly classified into reconfigurable and restructurable approaches. Numerous results have been proposed related to both approaches in the past few years.[2–5] One approach to design reconfigurable flight control systems is based on *a priori* knowledge of possible failures; the precomputed laws are calculated off-line and stored in the on-board memory, ready for on-line use whenever needed. The advantage of this approach is rapid adaptability, the disadvantage being extensive prior design usage of large memory space. An alternative approach is taken for restructurable schemes where flight controllers are calculated on-line using adaptation techniques. The benefit of this approach is that the control laws can cater to unforeseen failure scenarios. However, in this case computational power could be a critical factor, and hence, stability of the adaptive controller.

This paper presents a reconfiguration approach based on the *a priori* synthesis of a Linear Parameter Varying (LPV) controller. The fault signal generated by an FDI algorithm is formulated as a parameter on which the LPV controller is scheduled. The prime advantage of this approach is that the synthesis results in a single multivariable controller with stability and robustness guarantees for the closed-loop system.

The paper is organized as follows. Section 2 presents a brief introduction to LPV systems and control. The control design objectives and synthesis are presented in Section 3. In Section 4 simulation results are included. Some conclusions are drawn in Section 5.

2 LPV System and Control

LPV systems are characterized as linear systems whose coefficients depend upon time varying parameters. Consider the system

$$\begin{bmatrix} \dot{x}(t) \\ e(t) \end{bmatrix} = \begin{bmatrix} A(\rho(t)) & B(\rho(t)) \\ C(\rho(t)) & D(\rho(t)) \end{bmatrix} \begin{bmatrix} x(t) \\ d(t) \end{bmatrix}$$

where the parameter $\rho(t) \in \mathcal{P}$ is an *a priori* unknown bounded function of time with known bounds, and $\mathcal{P}$ is a set of functions that remain in a compact real subspace. If $\rho(t)$ is constant, we recover a linear time-invariant (LTI) system. An *ad hoc* method often used to derive gain-scheduled control for LPV systems is to design controllers for several fixed values of ρ using standard LTI control design techniques and combining the point designs — often with no stability guarantees at intermediate points.

The LPV control design problem is to generate a single control law which explicitly depends on the varying parameters. By guaranteeing that stability and performance criteria are met for all values of $\rho(t)$ within a

*Graduate Research Assistant, Department of Aerospace Engineering & Mechanics. Email: suvo@aem.umn.edu
†Graduate Research Assistant, Department of Aerospace Engineering & Mechanics. Email: marcosa@aem.umn.edu
‡Professor, Department of Aerospace Engineering & Mechanics. Email: balas@aem.umn.edu

given set of bounds, stability and performance of the parameter-varying closed-loop system can be guaranteed.

The LPV controller synthesis involves finding an output feedback controller $K(\rho)$ such that the closed loop system achieves exponential stability and the $\mathcal{L}_2$ norm of d to e is minimized. The synthesis problem can be posed as the following optimization

$$\min_{X(\rho),Y(\rho)} \gamma \tag{1}$$

subject to a set of linear, matrix inequalities (LMIs).[6,7] The state-space representation of the LPV controller $K(\rho)$ is constructed from the solutions $X(\rho)$ and $Y(\rho)$ of the LMI optimization problem.

3 Reconfigurable LPV Control Design

This section presents a reconfigurable LPV control design for the Boeing 747-100/200 longitudinal axis which schedules on a fault signal from FDI module monitoring the health of the elevator actuator. The LPV controller also schedules on altitude and velocity to provide stability and performance over the Up-and-Away flight envelope. The control design objectives are presented in Section 3.1. In Section 3.2 an LPV controller is synthesized across the flight regime assuming no fault in the elevator actuator. Section 3.3 presents an LPV control design assuming a full elevator fault and uses stabilizer as the alternative control surface for flight maneuvers. Section 3.4 presents the reconfigurable LPV control design.

3.1 Control Design Objectives

The primary control objectives are to obtain decoupled tracking of flight-path angle (FPA) and velocity over the entire Up-and-Away flight envelope. The tracking responses should be smooth and with settling times of 20 sec and 45 sec for flight-path angle and velocity respectively, with the elevator surface fully functional. With elevator control failure, the controller should stabilize the closed-loop system though with a less responsive flight-path angle tracking response. The settling time for the faulted FPA response is chosen as 30 sec — a one-third reduction in tracking responsiveness compared with the non-faulted case. The velocity tracking objective in the presence of an elevator fault remains unchanged since velocity is primarily controlled by thrust. In addition to the tracking objectives, the controller should have good gust disturbance rejection properties.

The longitudinal axis quasi-LPV aircraft model used for design has four states:[8,9] pitch rate q (deg/s), longitudinal velocity V (m/s), angle-of-attack α (deg) and pitch angle θ (deg). The altitude h (m) being a derived state is not used for control design. There are three control inputs: elevator deflection δ_e (deg), stabilizer deflection δ_s (deg) and thrust T (N). The measurements available are FPA γ (deg), acceleration $\dot{V}$ (m/s^2/g), pitch angle (deg), pitch rate (deg/s) and velocity (m/s).

The deflection and rate limits for the elevator are -23 to 17 deg and ± 37 deg/s respectively as specified in reference.[10] For the stabilizer the position and rate limits are -12 to 3 deg and 0.5 deg/s respectively. Accounting for the rate limits, the elevator and stabilizer are modeled as simple first-order transfer functions: $37/(s+37)$ and $0.5/(s+0.5)$ respectively. The engine is modeled as $0.5/(s+0.5)$ based on the engine transient characteristics provided in reference.[10] The maximum available thrust and thrust rate are 167,000 N and 83,500 N/s respectively.

The Up-and-Away flight envelope is defined by altitude and velocity ranges. The altitude varies from 4000 m to 8500 m. The velocity varies from 184 m/s to 280 m/s at 4000 m and 211 m/s to 280 m/s at 8500 m. The two velocity ranges define the trimmable region for straight-level flight in the given altitude range. The resulting flight envelope is trapezoidal in shape as shown in Figure 1. It is desired to synthesize LPV controllers for this flight envelope with altitude and velocity as scheduling parameters. The LPV synthesis software algorithms used in this research requires a rectangular gridded parameter space. Hence, the trapezoidal region in (h, V) coordinates is transformed to a rectangular region in (h, V_s) using the mapping

$$V_s = 280 - \frac{20,000}{20,000 - h}(280 - V) \text{ for } 160 \text{ m/s} \leq \text{V} \leq 280 \text{ m/s}, \; 4{,}000 \text{ m} \leq \text{h} \leq 8{,}500 \text{ m}.$$

Hereafter, V_s denotes synthetic velocity. Thus, in Figure 1, point '1' ($h = 4,000$ m, $V = 184$ m/s) is represented by ($h = 4,000$ m, $V_s = 160$ m/s) in the rectangular coordinate system.

3.2 LPV Controller for No Elevator Fault (K_{NF})

The LPV control design for no elevator failure is presented in this section. The scheduling parameters chosen for the LPV control design are altitude, h, and synthetic velocity, V_s. The velocity and FPA tracking problems are formulated as a model matching problem in the LPV control synthesis framework. For FPA response, the ideal transfer function T_γ for normal operation is modeled as a second order system, $\frac{0.35^2}{(s^2 + 2 \cdot 1 \cdot 0.35s + 0.35^2)}$, having a cut-off frequency at 0.35 rad/sec and damping factor of 1.0. The time response of the selected T_γ has a settling time of 20 sec. The ideal transfer function for velocity tracking T_V during normal operation is also modeled as a second order system, $\frac{0.15^2}{(s^2 + 2 \cdot 1 \cdot 0.15s + 0.15^2)}$ with 0.15 rad/sec natural frequency and critical damping and having a settling time of 45 sec.

The interconnection structure for the LPV control design is shown in Figure 2. To reduce the state-order of the weighted open-loop system and reduce computation time, sensor model dynamics are ignored for control design. The input scaling weight, W_{scl}, normalizes the reference inputs to the maximum expected commands.

W_{scl} is selected as diag (3/57.3,10) which corresponds to a 3 deg FPA command and 10 m/s velocity command.

The performance weighting function, W_p, has diagonal entries only and penalizes the FPA and velocity error. Both performance weights for FPA and velocity are chosen as $\frac{100(s/100+1)}{(s/0.005+1)}$. These correspond to an allowable tracking error of less than 1% at low frequencies for the FPA and velocity responses. The performance requirements roll off with increasing frequency and have a cross-over frequency at 0.5 rad/s. Unmodeled dynamics of the aircraft are taken into account using the multiplicative uncertainty weight W_u. W_u is a diagonal matrix with diagonal entries as $\frac{0.1(s/0.5+1)}{(s/100+1)}$ corresponding to the elevator and thrust channels. The weights are used to account for potential modeling error of 10% at low frequencies. The uncertainty weight rolls up at higher frequencies to limit the controller bandwidth and account for increasing model error at higher frequencies and has a cross-over frequency at 5 rad/s. W_n is selected as a diagonal matrix which accounts for sensor noise models in the control design. A constant noise weight of 0.01 is chosen for the FPA measurement. The noise weights for the other measurements are chosen to be frequency-dependent: $\frac{0.1}{g}\frac{(s/0.5+1)}{(s/100+1)}$ for $\dot{V}/g$, $\frac{0.05(s/0.5+1)}{(s/100+1)}$ for both θ and q, and $\frac{0.05(s/0.5+1)}{(s/100+1)}$ for V. These represent noise levels of $0.1/g$ for $\dot{V}/g$, 0.05 deg for θ, 0.05 deg/s for q and 0.05 m/s for V at low frequencies. The noise in each of these measurements increases at higher frequencies.

For the interconnection structure in Figure 2, $\mathcal{H}_\infty$ controllers are synthesized for several trim-points in the flight envelope. The spacing of the grid points was selected based upon how well the $\mathcal{H}_\infty$ point designs perform for plants around the design point. A 3×4 set of grid-points were selected for the $h \times V_s$ design space as shown in Figure 1.

To solve the LPV synthesis problem, basis functions are chosen for the LMI solutions $X(\rho)$ and $Y(\rho)$. Currently, there is no analytical method to choose the basis functions. In this case, several power series sets are tested and finally a second order power series $\{1, \rho^2\}$ of the scheduling parameters is chosen based on the lowest closed-loop $\mathcal{L}_2$ norm achieved. The rate limits of variation of the scheduling parameters are chosen as ± 25 m/s for h and ± 2 m/s^2 for V_s. These represent a maximum deviation of 25 m/s in vertical speed and $0.2g$ in acceleration. The final LPV controller obtained (K_{NF}) has 19 states and achieves a closed-loop induced $\mathcal{L}_2$ norm of 1.24.

K_{NF} is simulated in the full nonlinear longitudinal model of the Boeing 747. A set of 3 deg FPA steps and 10 m/s velocity steps are issued to the controller to fly the aircraft from grid-point '1' (h = 4000 m, V_s = 160 m/s) to near grid-point '12' (h = 8500 m, V_s = 280 m/s) as shown in Figure 1, the two extreme grid-points in the flight envelope. The dashed lines in Figure 4 show the state and actuator responses. It is observed that steady state tracking of the FPA and velocity commands are obtained over the flight envelope. The actuator responses are within limits.

3.3 LPV Controller for Full Elevator Fault (K_F)

This section presents the LPV control design with a full fault of the elevator. Analyzing the frequency responses of the control inputs to the measurements, it is observed that the low frequency stabilizer channel gains are higher than the elevator channel gains by a factor of 2 for the entire flight regime. Hence, for the purpose of controller synthesis, the same interconnection structure as for the previous design is used with the elevator dynamics replaced by the stabilizer dynamics. While performing simulations, commands are issued to the stabilizer path with a gain factor of 1/2 at the output of the controller.

Since the stabilizer dynamics are slower than the elevator dynamics, the desired FPA tracking response is slowed. T_γ is chosen as $\frac{0.25^2}{(s^2+2\cdot 1\cdot 0.25s+0.25^2)}$, with the cut-off frequency changed from 0.35 to 0.25 rad/sec. This corresponds to a settling time of 30 sec for FPA response. The performance weight for FPA tracking is changed to $\frac{100(s/100+1)}{(s/0.0035+1)}$ which has a lower cut-off frequency at 0.35 rad/s than that of K_{NF}. All other weighting functions and basis functions for LPV control design are kept the same as presented in Section 3.2. The synthesized LPV controller (K_F) has a state-order of 19, and a closed-loop induced $\mathcal{L}_2$ norm of 1.89.

Nonlinear simulations are performed for the same set of commands as in Section 3.2 with K_F. The solid lines in Figure 4 show the state and actuator responses for the closed-loop simulation. Decoupled command tracking is obtained for the FPA and velocity command sets over the flight regime. The FPA response responsiveness is decreased from a 20 sec settling time to 30 sec settling time. The engine and stabilizer control actions are slower compared to K_{NF} resulting in the slower FPA response.

3.4 LPV Controller with Fault-Scheduling (K_R)

This section presents the reconfigurable LPV control design which schedules on a fault/no-fault signal obtained from an FDI filter, in addition to altitude and synthetic velocity. The idea is to combine the two designs presented before, K_{NF} and K_F.

Let ρ_f represent the FDI signal. It is assumed that for a fully functional elevator, the FDI algorithm generates $\rho_f = 0$, while for a faulted elevator, it returns $\rho_f = 1$. In a realistic scenario, the signal from an FDI filter will be corrupted with noise, so it is assumed that ρ_f is the output of a logic switch which gets triggered when the filter signal crosses a minimum threshold level.

From the control synthesis point of view, the difference between K_{NF} and K_F is in the selection of ideal models

for FPA tracking (T_γ) and corresponding performance weighting functions ($W_{p\gamma}$). All other weighting functions are same. Thus, designing K_R requires T_γ and $W_{p\gamma}$ to be scheduled on ρ_f. $T_\gamma(\rho_f)$ is chosen as $\omega(\rho_f)^2/(s^2 + 2 \cdot 1 \cdot \omega(\rho_f)s + \omega(\rho_f)^2)$ where $\omega(\rho_f)$ is a linear function of ρ_f such that at $\rho_f = 0$, $\omega(\rho_f) = 0.35$ and at $\rho_f = 0$, $\omega(\rho_f) = 0.25$. Thus, $T_\gamma(0)$ represents the ideal FPA tracking model for K_{NF} while $T_\gamma(1)$ represents the same for K_F. Similarly, $W_{p\gamma}(\rho_f)$ is chosen as $\frac{100(s/100+1)}{(s/\omega(\rho_f)+1)}$ such that the function values at $\rho_f = 0$ and 1 represent the FPA performance weight for K_{NF} and K_F respectively while for intermediate values of ρ_f, the cut-off frequency $\omega(\rho_f)$ is interpolated linearly. The elevator and stabilizer channels are augmented with gains $(1-\rho_f)$ and ρ_f (Figure 3) to represent control allocations. Thus, for $\rho_f = 0$ only the elevator is used while for $\rho_f = 1$ the stabilizer provides the control. During synthesis, the elevator and stabilizer outputs are added to provide elevator command. This is done because an interconnection where the elevator and stabilizer commands are fed directly to the plant leads to counter-action of the control surfaces. During simulations, the stabilizer command is directly supplied to the plant with a gain of 1/2 since the open-loop stabilizer and elevator paths differ by a factor of 2.

The grid points for ρ_f are chosen as [0,0.5,1] and max $(\dot{\rho_f})$ as ± 1 sec^{-1}. The rate bound on ρ_f implies that the controller requires a reconfiguration time of at least 1 sec. The basis functions for the LMI solutions ($X(\rho)$ and $Y(\rho)$) are selected as the second order power series $\{1, \rho^2\}$ of the scheduling parameter. The synthesized controller has 19 states and achieve a closed-loop induced $\mathcal{L}_2$ norm of 2.39. Nonlinear simulations for different elevator fault scenarios are performed and the results are discussed in the next section.

4 Reconfiguration Simulation

Typical nonlinear actuator failures include: (1) freezing or lock-in-place; and (2) float.[5] Freezing corresponds to the control effector locked in a particular position and not responding to further commands. A float failure corresponds to the control surface floating about its zero moment position, thus becoming ineffective.

Nonlinear simulations for the B-747 are performed with the above failure scenarios of the elevator. In case of the both type of failures, it is assumed that an instantaneous fault detection signal is available. Based upon the FDI signal, the LPV controller reconfigures itself in 1 sec to use the stabilizer once the elevator fault occurs. The trim flight conditions chosen for the fault simulations are given by an altitude of 7,000 m and velocity of 241 m/s (grid point '8').

4.1 Lock-type Failure

A lock-type of failure is considered in the elevator actuator during a climb maneuver of the aircraft. To simulate the lock-type failure, a 3 deg FPA step command is issued to the controller from 5 sec to 30 sec, and the elevator is locked in its position at 10 sec. Figure 5 shows the aircraft responses for the elevator-lock scenario (dashed-line) and is compared with the responses during normal operations (solid-line). An overshoot of 0.5 deg is observed in the FPA response which dies out in 15 sec and there is negligible coupling in velocity response. Thus, the stabilizer is able to trim out the constant disturbance acting in the locked elevator channel. It is also observed from the step command at 30 sec that the FPA response is slowed after the occurrence of the fault and the settling time is increased from 20 sec to 30 sec as specified in the control design.

4.2 Float-type Failure

To simulate a float-type failure in the elevator, the elevator control signal is replaced with the angle-of-attack of the aircraft. This essentially simulates an ineffective elevator actuator that is unable to generate moment. Simulations are performed for a 3 deg FPA step command starting from 5 sec up to 30 sec. The fault occurs at 10 sec. The aircraft responses are plotted in Figure 6. An initial transience of 0.5 deg is observed in the FPA response and the coupling to velocity is minimal. The reconfigured controller stabilizes the aircraft after the elevator-float and provides a slower performance in terms of the FPA command response as contemplated during the control design stage.

4.3 Disturbance Rejection

One of the performance objectives of the reconfigurable LPV control design was that the controller should also have good disturbance rejection characteristics, in addition to decoupled command tracking properties. The LPV controller is simulated with sensor noise and wind gusts during a lock-type elevator failure at an altitude of 7000 m and trim velocity of 241 m/s and the aircraft responses are presented here. A light wind gust is chosen for simulation, which corresponds to a statistical probability of exceedance of 10^{-2}.[11] The sensor measurements are corrupted with white noise with the following maximum levels: ± 0.1 deg for γ, ± 0.05 g for $\dot{V}$, ± 0.1 deg for θ, ± 0.05 deg/s for q and 0.5 m/s for V. These correspond to a noise-to-signal ratio of 5-10% of the measurements. The nonlinear simulations are plotted in Figure 7. It is observed that decoupled command tracking of FPA and velocity is achieved both before and after the occurrence of the elevator failure in the presence of the sensor noise and turbulence. The deviations of the aircraft states are minimal when compared to those for no disturbance input. The elevator and stabilizer rates are within their rate saturation limits of ± 37 deg/s and ± 0.5 deg/s respectively (not shown).

5 Conclusion

In this paper LPV control design techniques are extended to control reconfiguration for elevator faults in the B-747 longitudinal axis. Simulations are performed with two elevator fault scenarios and the results show that stability, desired tracking and good disturbance rejection are obtained both before and after control reconfiguration.

Acknowledgements

This research was supported under NASA Langley Cooperative Agreement No. NCC-1-337. The technical monitor is Dr. Christine Belcastro.

References

[1] NASA Website, `http://avsp.larc.nasa.gov/`.

[2] Moerder, D.D., Halyo, N., Broussard, J.R., and Caglayan, A.K., "Applications of Precomputed Control Laws in Reconfigurable Aircraft Flight Control System," *Journal of Guidance, Control, and Dynamics*, Vol. 12, No. 3, May-June 1989, pp. 325–333.

[3] Middleton, R.H., Goodwin, C.G., Hill, D.J., and Mayne, D.Q., "Design Issues in adaptive control," *IEEE Transactions on Automatic Control*, Vol. 33, No. 1, January 1988, pp. 50–58.

[4] Napolitano, M.R., Song, Y., and Seanor, B., "On-line paramter estimation for restructurable flight control systems," *Aircraft Design*, Vol. 4, No. 1, March 2001, pp. 19–50.

[5] Bošković, J.D. and Mehra, A., "Stable Multiple Model Adaptive Flight Control for Accomodation of a Large Class of Control Effector Failures," *Proceedings of the American Control Conference*, San Diego, California, June 1999, pp. 1920–24.

[6] Wu, F., *Control of Linear Parameter Varying Systems*, Ph.D. thesis, Department of Mechanical Engineering, University of California at Berkeley, 1995.

[7] Shin, J.Y., *Wost-Case Analysis and Linear Parameter-Varying Gain-Scheduled Control of Aerospace Systems* , Ph.D. thesis, Department of Aerospace Engineering and Mechanics, University of Minnesota, 2000.

[8] Marcos, A., *A Linear Parametric Varying Model of the Boeing 747-100/200 Longitudinal Motion*, Master's thesis, Department of Aerospace and Engineering Mechanics, University of Minnesota, January 2001.

[9] Marcos, A. and Balas, G., "Linear Parameter Varying Modeling of the Boeing 747-100/200 Longitudinal Motion," *AIAA 2001 Guidance, Navigation, and Control Conference, AIAA-01-4347*, Montreal, Canada, August 2001.

[10] Hanke, C. and Nordwall, D., "The Simulation of a Jumbo Jet Transport Aircraft. Volume II: Modeling Data," Tech. Rep. NASA CR-114494/D6-30643-VOL-2, The Boeing Company, 1970.

[11] Marcos, A., Ganguli, S., and Balas, G., "A Linear Parameter Varying Fault Detection and Isolation Filter for the Boeing 747-100/200," to be published.

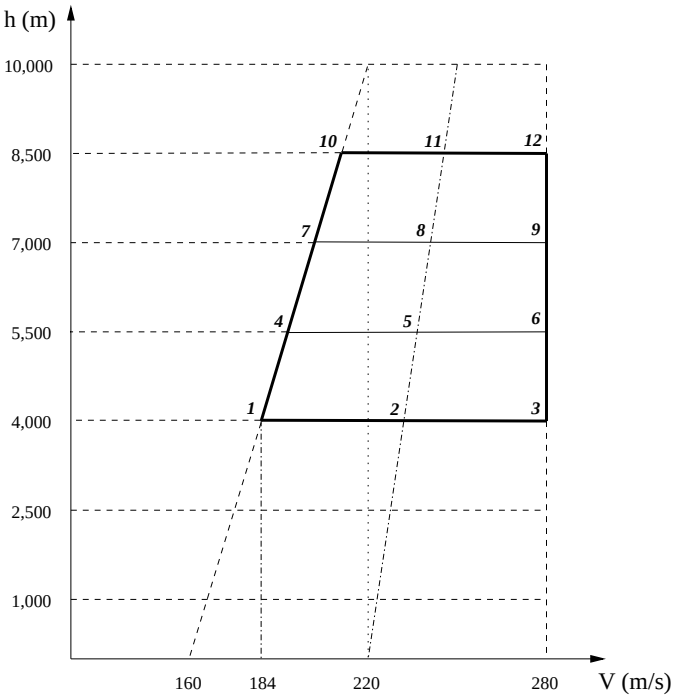

Figure 1: B-747 Up-and-Away flight envelope — trapezoidal area enclosed by bold lines.

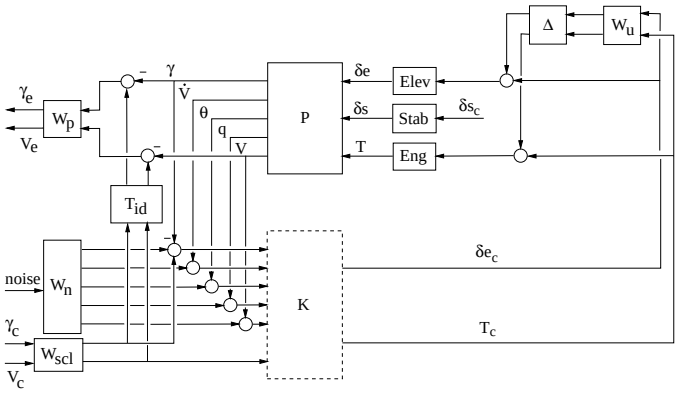

Figure 2: Interconnection structure for K_{NF} and K_F.

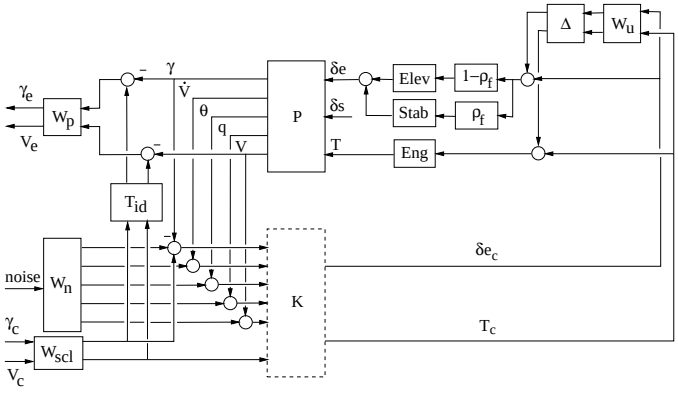

Figure 3: Interconnection structure for K_R.

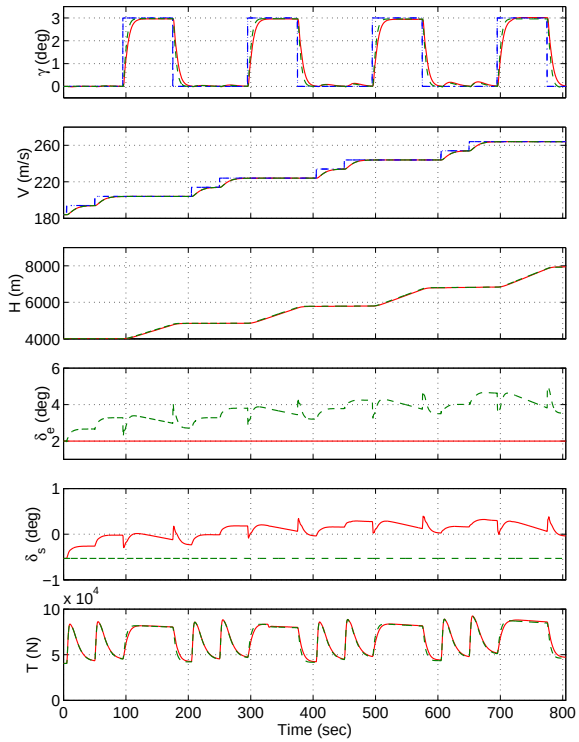

Figure 4: Aircraft responses for LPV controller during normal operation (K_{NF} - dashed) and with full elevator fault (K_F - solid). Commands are in dashdot lines.

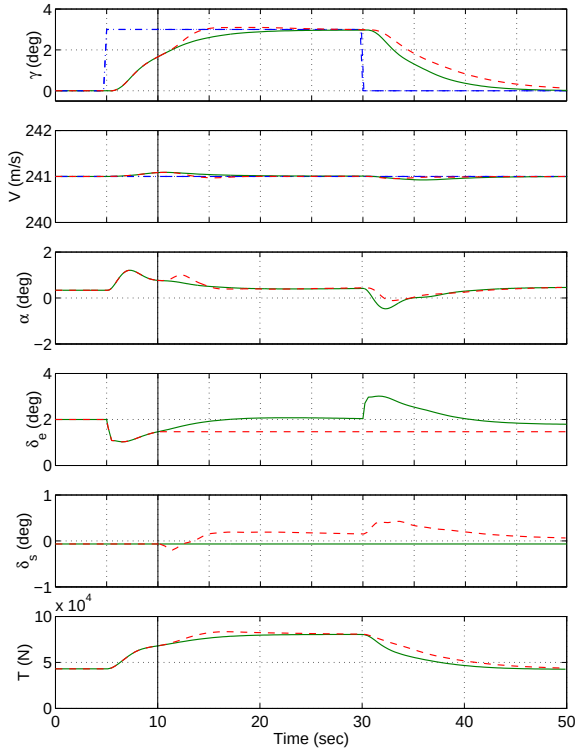

Figure 5: Aircraft responses for K_R with elevator-lock at 10 sec. (Commands: dashdot; normal: solid; locked: dashed).

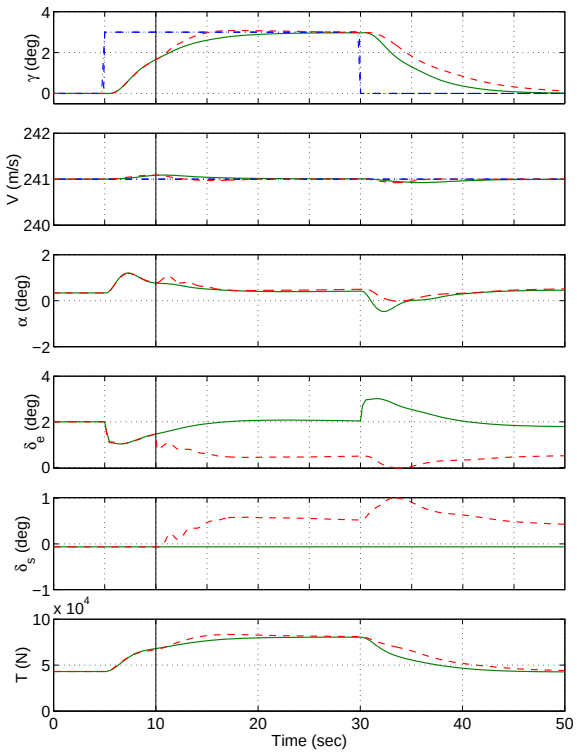

Figure 6: Aircraft responses for K_R with elevator-float at 10 sec. (Commands: dashdot; normal: solid; float: dashed).

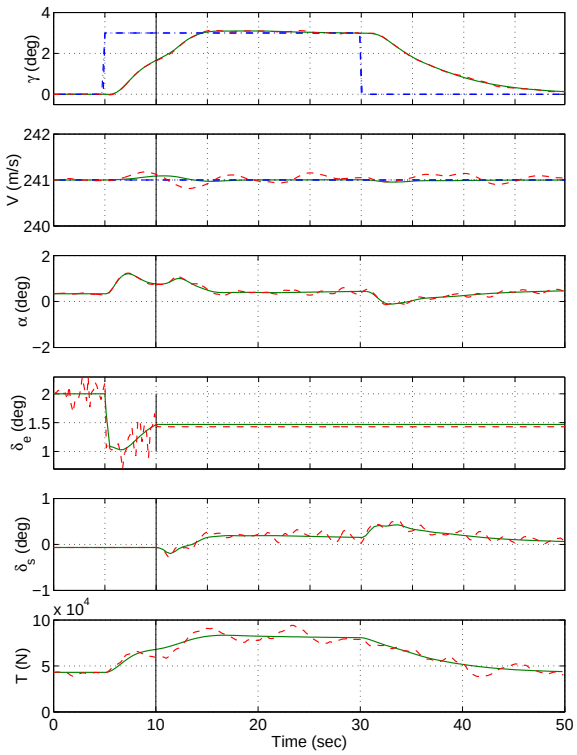

Figure 7: Aircraft responses for K_R with elevator-lock at 10 sec with sensor noise and wind gust. (Commands: dashdot; locked: solid; with disturbance: dashed).